Materials Research Proceedings 41 (2024) 576-585 https://doi.org/10.21741/9781644903131-64

Simulation and monitoring of the infusion of thick composites with thermoplastic acrylic resin

SIDDIG Nihad[1,a *], LE BOT Philippe[1,b], FOUCHÉ Olivier[1,c] and DENIS Yvan[1,d]

[1] Nantes Université, IRT Jules Verne, 1 Mail des 20 000 Lieues, 44340 Bouguenais, France

[a]nihad.siddig@irt-jules-verne.fr, [b]philippe.lebot@irt-jules-verne.fr,
[c]olivier.fouche@irt-jules-verne.fr, [d]yvan.denis@irt-jules-verne.fr

Keywords: Composites, Thermoplastic, Monitoring, Simulation, Polymerization

Abstract. The ZEBRA project aims to advance the circular economy by creating wind turbine blades that can be completely recycled. Currently, Wind turbine blades are fabricated through Vacuum-Assisted Resin Infusion (VARI) using thermoset resins. In this endeavor, the recyclable thermoplastic resin Elium® from Arkema is utilized as a sustainable alternative to traditional thermoset resins. The production of thick and sizable components using reactive resins presents various intertwined physical aspects and difficulties, notably concerning potential overheating during the Elium® radical polymerization process. The optimization of this process necessitates the use of simulation to save the expensive time and effort caused by the experiments. However, to be reliable, these numerical methods must be validated to allow accurate predictions for potential defects with thick and complex parts. The challenge lies in flow front detection in the through-thickness direction. In this work, infusion tests were conducted for thick parts in a testing bench instrumented with a robust monitoring system. QRS sensors are placed through the part thickness to detect the front arrival instantaneously. The simulations are compared and validated to the signals of the QRS sensors for validation. Then the model was used to predict the flow behavior for more complex parts. A 3D flow is observed by the differences in permeability between the flow medium and the fabric, which induces a high difference in resin arrival times to the sensors depending on the position of sensors through the part thickness. The flow simulations showed a good approximation of the experimental results. However, deviations are observed in the flow front position, caused by the disturbance induced by the presence of the sensors.

Introduction

The ZEBRA (Zero wastE Blade ReseArch) project, led by French research center IRT Jules Verne, gathers ARKEMA, CANOE, SUEZ, LM Wind Power, Owens Corning, and ENGIE, aims to manufacture 100 % recyclable wind turbine blades while being economically and environmentally feasible with a circular approach. Manufacturing wind blades typically involves the vacuum-assisted resin infusion (VARI) technique with thermoset resin. To overcome the recycling challenges of wind blade manufacturing [1], the project substitutes conventional thermoset resin with Elium® thermoplastic resin, developed by Arkema. LM Wind Power fabricated two 100% recyclable wind blades throughout the project's lifetime. The second recyclable wind blade with a carbon spar cap manufactured by LM Wind Power is shown in Figure 1. The vacuum-assisted resin infusion (VARI) process for wind blades can be intricate and variable, leading to defects in the final product [2]. Identifying risks and defects in the process is crucial for ensuring high-quality parts, traditionally done through time-consuming and costly experimental testing [3].

Figure 1: The second 100% recyclable ZEBRA 77m wind blade manufactured by LM Wind Power

To overcome the process challenges, numerical simulation models the manufacturing process, identifying potential risks impacting quality and cost [4][5]. However, for these numerical methods to be trustworthy, validation is crucial to enable accurate predictions for potential defects, especially in the case of thick and complex parts [6][7][8]. The difficulty lies in detecting the flow front in the through-thickness direction. In this study, infusion tests were carried out on thick parts using a testing bench equipped with a robust monitoring system [9]. Sensors are strategically placed throughout the part thickness to instantly detect the front arrival. The simulations were then compared and validated against the signals from the sensors for accuracy. Subsequently, the model was employed to predict the flow behavior for more complex parts. The paper investigates simulating thick continuous fiber/reactive thermoplastic resin composites for wind energy applications. The study aims to establish a solid foundation for process optimization, linking experimental characterization and numerical simulations, explore the use of QRS sensors in the flow front detection through the part thickness, compare two simulation strategies and cross-check these results with sensor acquisitions.

Experimental Characterization and Monitoring

This section presents the materials employed in the infusion process, the experimental approach and the monitoring system.

Materials

The thermoplastic resin Elium® developed by Arkema was used for its recyclability. Elium® is categorized as an acrylic reactive resin capable of producing large-scale fiber-reinforced plastics [10]. The resin undergoes free radical polymerization, where the catalyst, Butanox 50 peroxide at a 2% concentration, initiates the transformation of the monomer methyl methacrylate into poly methyl methacrylate. A 50/50 mixture of Elium® 191 SA and Elium® 191 XO was utilized for infusion experiments. This resin has a density of 1.01 g/cm3 and a viscosity of approximately 0.1 Pa.s at 23°C. To ensure precision, the dynamic viscosity of the resin is assessed using a flow cup, adhering to ISO 2431 standards. Composite panels were fabricated using a stack of Owens Corning high-performance unidirectional glass fabric, resulting in a panel measuring 600 mm in length, 300 mm in width, approximately 50 mm in thickness and 78 plies of fabric. To aid resin flow, the flow medium Infuplex OM 70, measuring 400 mm in width, 250 mm in length, and 1 mm in thickness, was employed. Permeability tests were previously conducted on both the reinforcement and distribution medium.

Experimental Bench

The experimental bench is used for conducting infusion tests on the presented components. The design and setup of this bench are critical factors influencing the reliability and accuracy of experiments. The features of the experimental bench are shown in Figure 2, shedding light on its role in facilitating controlled and representative conditions for the infusion process. In that

experimental bench, the tool is made of transparent glass, allowing resin front position acquisition at the lower tool side.

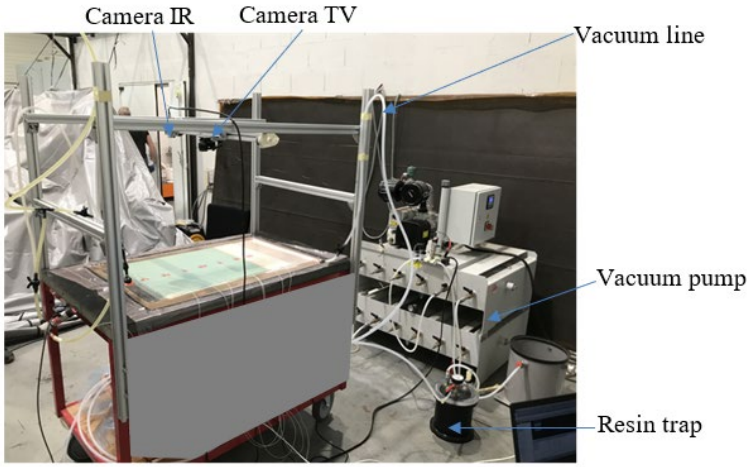

Figure 2: The infusion test bench

QRS sensors

The infusion process is closely monitored using Quantic Resistive sensors (QRS®) from SeNSE-IN, strategically positioned throughout the thickness of the material (Figure 3). QRS® sensors are nano-structured strain, transducing strain at the nanoscale into a macroscopic resistive signal for consumption of only some mW. That is why their first applications were initially dedicated to SHM objectives [11]. SeNSE-IN designs them now for process monitoring applications. They can be positioned on the surface or in the core of the composite material between plies (Figure 4), and they can be made of the same resin as the composite if necessary. The connection from active part sensors (with a surface area of about 1 cm^2) to the data acquisition system is guaranteed by 0.2 mm diameter copper wires.

These sensors play a crucial role in capturing and instantaneously detecting the arrival of the flow front during infusion tests. By being embedded throughout the part thickness, the QRS® sensors provide a comprehensive understanding of the infusion dynamics, offering real-time data on the progression of the resin through the material. This detailed monitoring not only enhances our ability to validate numerical simulations but also serves as a key element in ensuring the accuracy and reliability of the experimental outcomes.

Additional sensors enable a better understanding of the infusion process: a Keyence flow meter FD-XC2063 and a vacuum sensor (Balluff BSP00ZK).

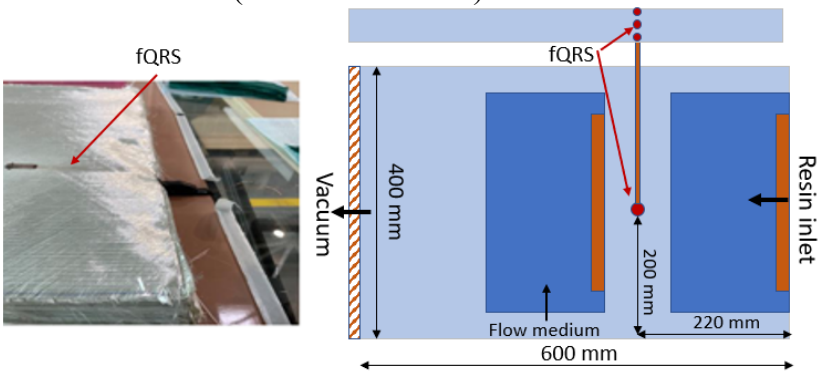

Figure 3: Sensor placement in the composite part, fQRS refers QRS sensors dedicated to flow measurement

Figure 4: Focus on Sensor integration in the composite part

Monitoring System for the Infusion Process

The infusion process monitoring is performed by two commercial systems. An HBM QuantumX 1601B device allows monitoring of the flow meter and vacuum sensor as well as some thermocouples in order to ensure the quality of the infusion process. A specific data acquisition system is dedicated to QRS© sensors. This QR-KUB® device, developed by SeNSE-IN, allows to visualize and store of up to 8 QRS sensor signals with 2 additive thermocouples (Figure 5).

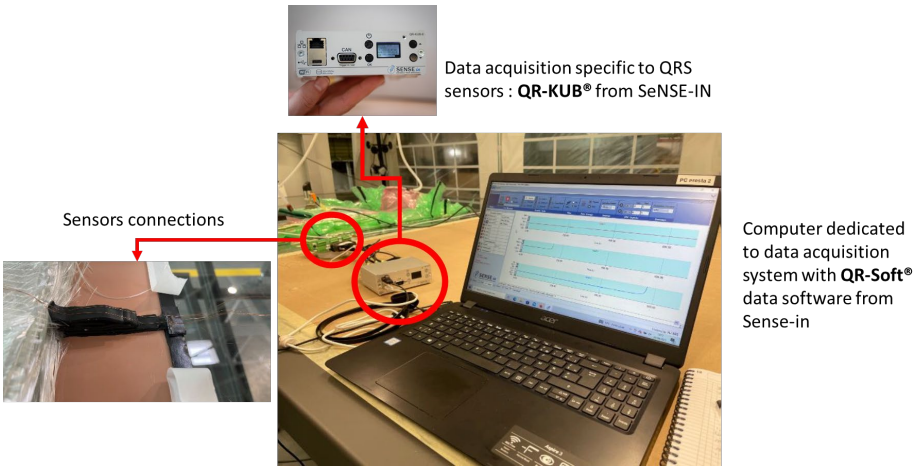

Figure 5: Data acquisition system

Modeling and Simulation

The infusion process combines several coupled physical phenomena: fluid mechanics represented in resin flow, thermal (transient heat transfer), chemical (resin polymerization kinetics), in addition to solid mechanics to model the potential deformation during and after impregnation (distortion) of the medium because of using flexible tooling. In this paper, the focus is drawn to resin flow, heat transfer and resin polymerization.

Simulation tool

The commercially available simulation software PAM-RTM® developed by ESI Group is used to simulate the infusion process. It is a Finite Element (FE) solution for modeling the manufacturing processes of structural and non-structural composites reinforced by continuous fibers. The software allows the coupling of the physical phenomena involved in the infusion process [9].

Boundary and initial conditions

Pressure Dirichlet boundary conditions are prescribed at the injection lines with the atmospheric pressure (Figure 7). The vacuum pressure of 0.2 bar is applied at the outlet along the opposite side. The initial temperature was assigned to the part and the mold. All the other surfaces subjected to natural convection boundary conditions.

Process physics

The flow of the incompressible fluid in the fibrous medium is governed, if the change of thickness is neglected, by the simplified form of the mass balance equation (Eq. 1) [12]:

$$\nabla \cdot (\vec{U}) = 0 \tag{1}$$

Where $\vec{U}$ is the liquid velocity. Darcy's law describes the flow of Newtonian fluids through porous media (Eq. 2); it relates the liquid velocity to the permeability tensor $\boldsymbol{K}$, the resin viscosity μ and the pressure gradient ∇P [13].

$$\vec{U} = \frac{-\boldsymbol{K}}{\mu} \nabla P \tag{2}$$

The energy balance equation (Eq. 3) governs the heat transfer problem. The terms of the energy balance equation on the left-hand side are, respectively from left to right: the transient and advection terms. On the right-hand side of the equation, the first part of the equation is the conduction term. The internal heat generation in the system is represented by $\dot{R}$ [14].

$$\rho\, c_p \frac{\partial T}{\partial t} + \rho_r c_{p,r} \vec{U} \cdot \nabla T = -\nabla \cdot (\lambda \cdot \nabla T) + \dot{R} \tag{3}$$

where T is the temperature, ρ and ρ_r are respectively the composite and the resin density. c_p and $c_{p,r}$ are the composite and the resin specific heat capacity, respectively. The subscript r denotes the resin. λ is the thermal conductivity of the composite material. The term $\dot{R}$ in the energy equation is the volumetric heat generation related to resin polymerization.

Results and Discussion

In this section, the key findings are presented and discussed, shedding light on the intricacies of resin infusion within thick components.

Sensor response analysis

The responses obtained from the QRS sensors provide crucial information about the dynamics of resin flow. The sensor data allows to identify patterns, anomalies, and correlations that contribute to a comprehensive understanding of the infusion dynamics through the part thickness. The comparison is only based on the resin arrival to the sensors, the curve is not considered.

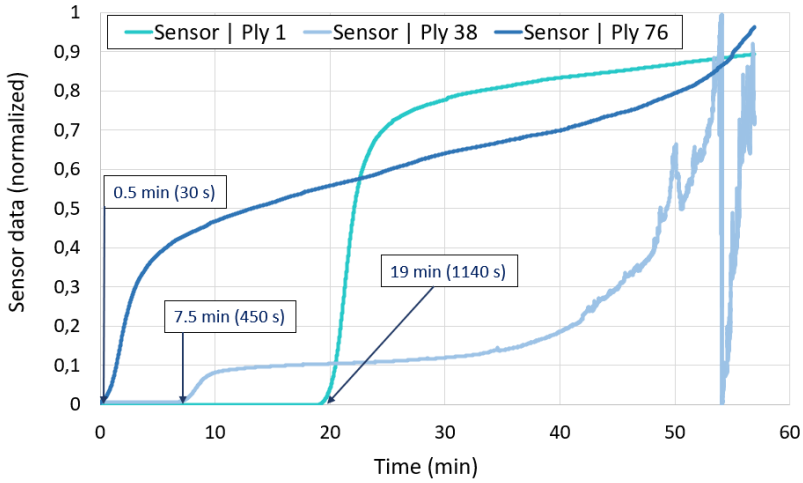

Figure 6: The sensor response in the experimental setting

Figure 6 plots the normalized sensor response in the three QRS sensors placed at different levels (Fig. 3). The sensor response is in Ohm, and it is normalized to the maximum value of each sensor. The three virtual sensors were placed at the same experiment positions: the first sensor above the ply in contact with the mold (ply 1), the second sensor at the central ply (38) and the last sensor under the upper ply (76). The first sensor detects resin right after the beginning of impregnation. This sensor is the nearest to the injection line and the flow medium which facilitates resin flow. The second sensor detects resin 7 minutes after the resin's arrival to sensor 1. The last sensor is the last sensor to detect the resin arrival, as the flow velocity decreases with time as it advances further than the distribution medium. This result shows that the variations in permeability between the flow medium and the fabric give rise to a substantial 3D flow.

Modeling and simulation of thick parts

The representation of the model is implemented using the PAM-RTM commercial tool to simulate the impregnation process. Similarly, to the infusion experiment, the part has a thickness of 50 mm with a sequential infusion through two infusion lines, two distribution media and one vacuum line. The two models are represented in Figure 7, the models are identical except for the meshing method through the part thickness. The first model, to the left, contains one element per ply. The model to the right (model 2), contains 10 elements as a total through the part thickness. The two models have the same number of in-plane elements. Representing one element per ply increases the model accuracy and its capacity to predict the flow front position with good precision. Reducing the number of elements to only 10 through the part thickness decreases the calculation time, but also deteriorates the precision. This study will help estimate the model simulation preferences to compromise and save cost and time along with having a good estimation of process physics. The sensor placement remains the same for the two models.

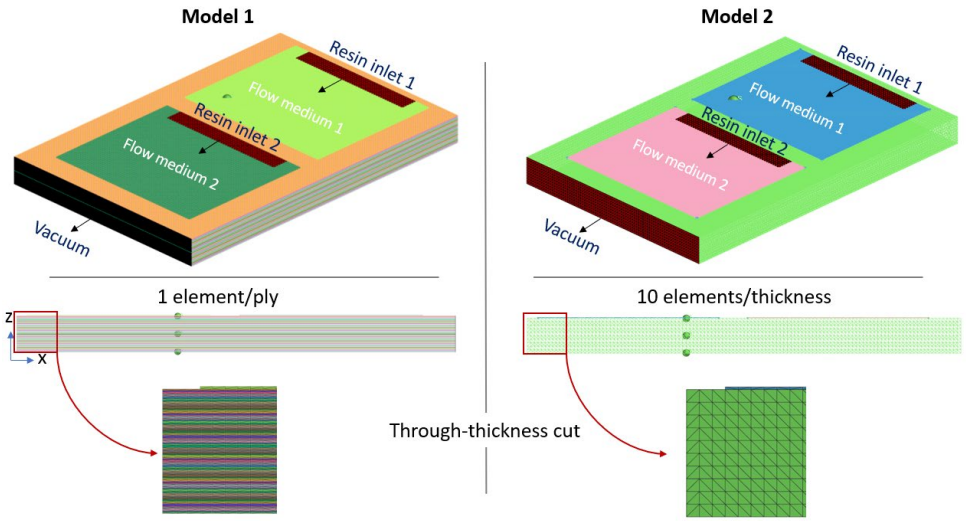

Figure 7: Numerical model implementation for thick parts

Figure 8 shows the flow front contours of the two models. The pattern seems to be similar for the models at the global dynamics shown by the upper contours, however, a slight difference in filling time is observed between the two models. The fewer the number of elements, the higher the filling time; this is due to the precision related to the difference in element numbers in the two models. The software homogenizes the permeability through each element with the second scenario, leading to an overestimation in the permeability value. Comparing two through-thickness sections at the same time instant (1011s), we observe faster impregnation and higher precision with the refined mesh of Model 1. These sections illustrate how thick parts substantiate the

influence of 3D flow especially in the presence of the distribution media, which induces differences in flow front velocities.

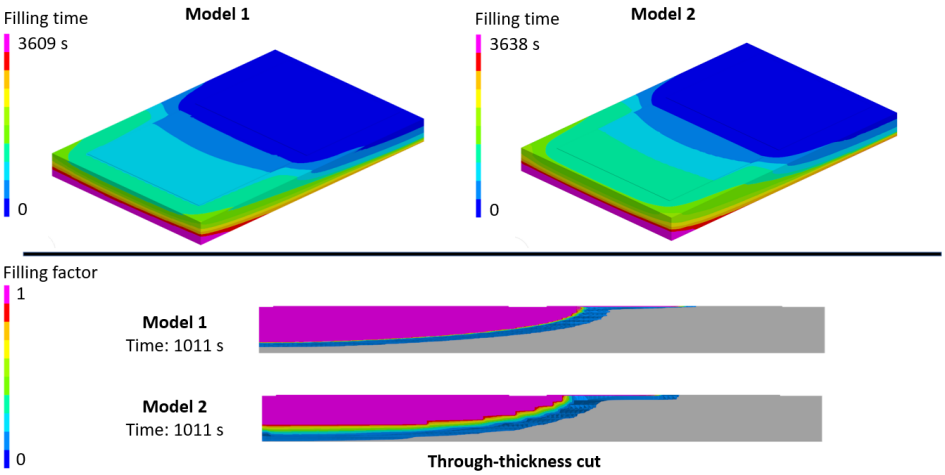

Figure 8: Filling comparison between model 1 and 2 in the in-plane and through-thickness directions

The three virtual sensors were placed at the same experiment positions. These sensors allow to follow the time evolution of pressure. The pressure is used as an indication of resin arrival, as a pressure rise is translated by resin arrival at the sensor.

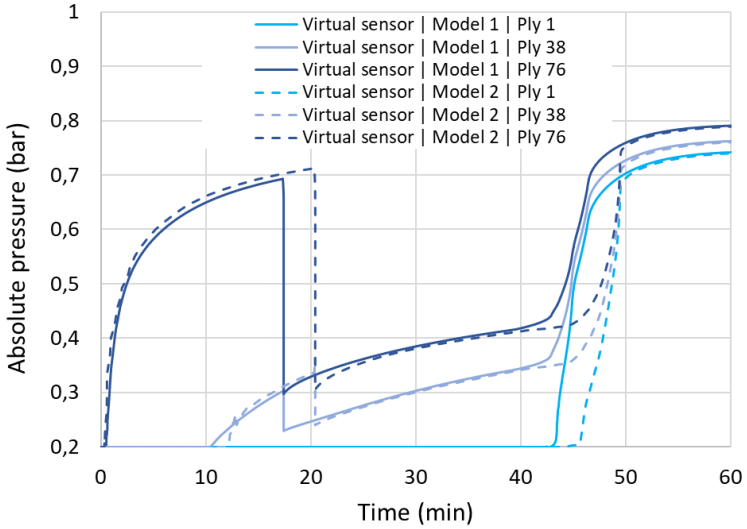

Figure 9: Pressure evolution with time at the virtual sensors

Figure 9 shows the pressure evolution with time at the three sensor locations for the two models. The continuous and dotted lines represent model 1 and model 2, respectively. A similar trend is observed between the two models, however, variations in resin arrival times are observed in the two models. Model 2 shows a lag of 2-4 minutes in resin detection time compared to model 1. Smooth curves are observed in Model 1, where higher precision is expected.

Comparison with experimental results

In the comparative analysis of numerical and experimental results, the sensor responses are a pivotal point of convergence. The data obtained from the QRS sensors during the infusion process is systematically compared with the predictions derived from numerical simulations regarding resin arrival time to sensors. This comparison allows us to assess the accuracy and reliability of the simulation models in replicating the dynamic behavior observed in the experimental setting.

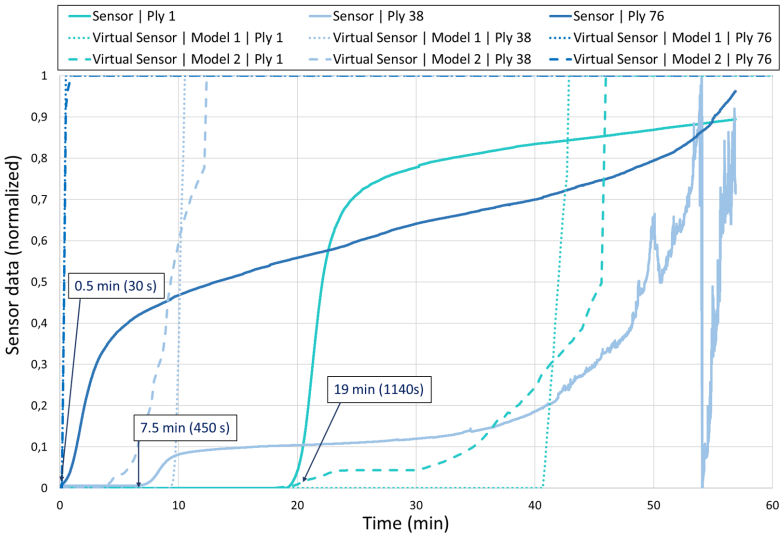

Figure 10: Comparison of senor acquisitions with simulation data

The comparison between the experimental sensor acquisitions and the numerical results is shown in Figure 10. The virtual sensor curves show the time evolution of the filling percentage (factor), varying from 0 to 1. In this figure, the continuous lines represent the normalized sensor signal. The virtual sensors are represented by the dotted lines (Model 1) and the dashed lines (Model 2). Generally speaking, the sensors detect the resin arrival earlier than the virtual sensors. This is because the QRS sensors have a wire that intrusively influences the resin flow. These wires create race-tracking channels, which transmit resin faster than the other parts of the fabric, leading to its arrival at a shorter time than the surrounding fabric. This influence is not observed by simulation, because the simulation does not consider the race-tracking induced by the sensor wire.

Comparing the two simulation strategies, Model 1 seems more accurate than Model 2 as the filling factor value of 1 at the complete sensor filling is more relevant to the experiment. Moreover, the virtual sensor response in Model 1 is smoother and disturbance-free. Model 2 seems to fluctuate under the influence of the insufficient number of through-thickness elements. At a macroscopic scale, the filling times are close, but the local dynamic is still very sensitive to the mesh size, for the same reasons explained before. Comparing the responses of the QRS, the virtual pressure and the filling factor sensors, it is observed that the QRS and the virtual filling factor sensors detect the flow front as soon as the resin reaches the sensor, and the signal evolves till the complete sensor filling. The pressure virtual sensors only detect the resin arrival when the sensor is 100% filled, resulting in a pressure rise. Care should be taken about the sensor choice for the monitoring of the infusion process. Vision camera is widely used to follow the in-plane flow front advancement. It is still challenging to control the infusion process in zones not covered by cameras, especially through the part thickness. When QRS sensors are used, the sensor acquisitions should be treated with special consideration. The resin detection time indicated by the sensor does not necessarily indicate the flow arrival to this specific zone of the part, because of the flow disturbance created by the sensor.

Conclusions

In this study, infusion tests were carried out on thick components using a testing bench equipped with a robust monitoring system. QRS sensors were strategically positioned across the thickness of the part to promptly identify the arrival of the front in the out-of-plane direction. The simulations were cross-referenced against the signals recorded by the QRS sensors for validation purposes. Two simulation models were presented, the difference lies in the number of elements through the part thickness. The finer mesh gave a more precise prediction of the experiment. The three QRS

sensors record significant differences in the arrival times of resin, depending on their location within the thickness of the part. These results shed light on the 3D flow variations induced by the permeability ratio between the flow medium and the fabric. The results of the flow simulations showed considerable discrepancies compared to the experimental findings, of about 2.5 min at sensor 2 and higher discrepancies at sensor 3, due to the flow disturbance created by the QRS sensors which generates race-tracking channels. These results provide valuable insights into the limitations of the sensors and highlight areas for potential improvement. This comprehensive evaluation of the numerical-experimental correlation not only contributes to the validation of the used approach but also guides the refinement of future models for a more accurate representation of the complex resin infusion dynamics within thick components. These findings can help address potential optimizations, challenges, and avenues for future research [15].

Acknowledgments
This study is a part of the ZEBRA project led by IRT Jules Verne (French Institute of Research and Technology in Advanced Manufacturing). The authors wish to thank the industrial partners of this project: LM Wind Power, Arkema, Owens Corning, ENGIE, Suez and CANOE and Ecole Centrale de Nantes, GeM laboratory.

References

[1] J. Beauson, A. Laurent, D. P. Rudolph, and J. Pagh Jensen, "The complex end-of-life of wind turbine blades: A review of the European context," *Renewable and Sustainable Energy Reviews*, vol. 155. Elsevier Ltd, Mar. 01, 2022. https://doi.org/10.1016/j.rser.2021.111847

[2] S. van Oosterom, T. Allen, M. Battley, and S. Bickerton, "An objective comparison of common vacuum assisted resin infusion processes," *Compos Part A Appl Sci Manuf*, vol. 125, 2019. https://doi.org/10.1016/j.compositesa.2019.105528

[3] N. Siddig *et al.*, "Infusion and Polymerization of Thick Glass/Elium® Acrylic Thermoplastic Resin Composites," in *ICCM23, Belfast, Ireland*, 2023. Accessed: Jan. 11, 2024. [Online]. Available: https://www.researchgate.net/publication/373049008_Infusion_and_Polymerization_of_Thick_GlassEliumR_Acrylic_Thermoplastic_Resin_Composites

[4] B. Liu, S. Bickerton, and S. G. Advani, "Modelling and simulation of resin transfer moulding (RTM)-gate control, venting and dry spot prediction," *Compos Part A Appl Sci Manuf*, vol. 27, no. 2, pp. 135–141, 1996.

[5] Carlone, P., Rubino, F., Paradiso, V., & Tucci, F. (2018). "Multi-scale modeling and online monitoring of resin flow through dual-scale textiles in liquid composite molding processes". The International Journal of Advanced Manufacturing Technology, 96, 2215-2230.

[6] P. Le Bot *et al.*, "Anomaly detection during thermoplastic composite infusion: Monitoring strategy through thermal sensors," in *Key Engineering Materials, Achievements and Trends in Material Forming*, vol. 926, 2022, pp. 1423–1436. https://doi.org/10.4028/p-n27w97

[7] Y. Denis, N. Siddig, R. Guitton, P. Le Bot, A. De Fongalland, and D. Lecointe, "Thermo-chemical modeling and simulation of glass/Elium® acrylic thermoplastic resin composites," in *ESAFORM, 19-21 April 2023, Kraków, Poland*. https://doi.org/10.21741/9781644902479-34

[8] Aleksendrić, D., Bellini, C., Carlone, P., Ćirović, V., Rubino, F., & Sorrentino, L. (2019). "Neural-fuzzy optimization of thick composites curing process". Materials and Manufacturing Processes, 34(3), 262-273.

[9] N. Siddig *et al.*, "Modeling and simulation of the fabrication of glass/elium® acrylic thermoplastic resin composites by the infusion process," *SAMPE Europe, Hamburg, Germany*, 2022.

[10] S. F. Gayot, C. Bailly, T. Pardoen, P. Gérard, and F. Van Loock, "Processing maps based on polymerization modelling of thick methacrylic laminates," *Mater Des*, vol. 196, p. 109170, 2020. https://doi.org/10.1016/j.matdes.2020.109170

[11] A. Lemartinel, M. Castro, O. Fouché, J. C. De Luca, and J. F. Feller, "Strain mapping and damage tracking in carbon fiber reinforced epoxy composites during dynamic bending until fracture with quantum resistive sensors in array," *Journal of Composites Science*, vol. 5, no. 2, 2021. https://doi.org/10.3390/jcs5020060

[12] C. H. Park, "Numerical simulation of flow processes in composites manufacturing," in *Advances in Composites Manufacturing and Process Design*, Woodhead Publishing, 2015, pp. 317–378. https://doi.org/10.1016/B978-1-78242-307-2.00015-4

[13] M. Deléglise, C. Binétruy, and P. Krawczak, "Solution to filling time prediction issues for constant pressure driven injection in RTM," *Compos Part A Appl Sci Manuf*, vol. 36, no. 3, pp. 339–344, 2005. https://doi.org/10.1016/j.compositesa.2004.07.001

[14] L. Shi, "Heat Transfer in the Thick Thermoset Composites, PhD Thesis, Delft University of Technology," Delft University of Technology, 2016.

[15] Boisse, P., Akkerman, R., Carlone, P., Kärger, L., Lomov, S. V., & Sherwood, J. A. (2022). "Advances in composite forming through 25 years of ESAFORM". International Journal of Material Forming, 15(3), 39.